Radiation Constrained Fair Wireless Charging

Lanlan Li*†, Haipeng Dai*, Guihai Chen*, Jiaqi Zheng*, Yang Zhao*, and Pengxiang Zeng‡
*State Key Laboratory for Novel Software Technology, Nanjing University, Nanjing, Jiangsu 210023, CHINA
†Department of Information Engineering, Nanhang Jincheng College, Nanjing, Jiangsu 211156, CHINA
‡School of Internet of Things Engineering, Jiangnan University, Wuxi, Jiangsu 214122, CHINA
{lanlanli,yangzhao}@smail.nju.edu.cn, {haipengdai,gchen}@nju.edu.cn, jiaqi369@gmail.com, 1030414329@vip.jiangnan.edu.cn

***Abstract*—Recently wireless power transfer technology (WPT) attracts considerable attention, its incurred electromagnetic radiation (EMR), however, is largely overlooked by most existing literatures. In this paper, we first propose and study the radiation constrained fair wireless charging problem, *i.e.*, maximizing the minimum utility of devices by adjusting the power of wireless chargers with no EMR intensity at any location in the field exceeding a given threshold R_t. To address this problem, we first adopt an area discretization method to transform it from nonlinear to linear. Then, we propose two algorithms to deal with the reformulated problem. One is called Primal-Dual algorithm, which is semi-distributed and uses lagrangian dual and sub-gradient methods to solve the problem iteratively. The other is called area division algorithm. It is not only fully distributed and scalable with network size, but also provably achieves an approximation ratio of $(1-\epsilon)$. We conducted extensive simulations and built a field test-bed to verify our theoretical findings. Our simulations show that the approximation ratio of the area division algorithm holds; the Primal-Dual and area division algorithms can have comparable and over 90.9% performance of the optimal results, respectively; and both of the algorithms outperform a baseline algorithm by more than 37%.**

I. Introduction

Nowadays, Wireless Power Transfer technology (WPT) has been attracting increasing attention around the world for its convenience and reliability. WPT can wirelessly provide energy for a great variety of consuming end-devices, such as RFIDs [1], sensors [2], cell phones [3], laptops [4], electric vehicles [5], wearables [6]. According to a report, the global wireless charging market is expected to reach nearly US$9.95 billion in 2018 [7].

There are lots of research works studying energy charging efficiency (*e.g.*, [8]–[13]). However, most of these works neglect one critical issue for WPT, that is, the safety of electromagnetic radiation (EMR). High EMR has been widely recognized as a threat to human health. It causes risks of diseases such as mental diseases, tissue impairment, and brain tumor. It is even more dangerous and harmful to pregnant women and children [14]. A few researchers [14]–[18] have taken care of EMR safety caused by WPT over the past few years. These works consider charging issues under the prerequisite of guaranteeing EMR safety, and most of them aim to maximize the overall charging utility of devices. However, this optimization goal may be not suitable for all the application scenarios. First, some devices may become victims under such schemes and receive low or even none charging power. They may keep in such energy-hungry status for a long time, which could heavily disrupt their normal operation. Second, the incurred charging unfairness could downgrade the overall performance of the whole network composed by the rechargeable devices. For instance, for wireless rechargeable sensor networks [8], the network lifetime is defined as the time duration from the starting time of the network to the time point when there is a sensor node that begins to run out its energy. Therefore, it is often desirable to achieve charging fairness in order to elongate the network lifetime for wireless rechargeable sensor networks. In this paper, we for the first time consider the charging fairness of rechargeable devices under EMR constraints. In particular, our goal is to maximize the minimum charging utility among all devices in the network with no location of the field exceeding the EMR safety threshold.

There are some literatures considering the EMR safety in studying charging efficiency issue. Most of these literatures concentrate on optimizing the overall charging utility of devices. For example, [14], [15] maximize the total utility of all the devices in the network. To the best of our knowledge, none of the existing literatures considers the charging fairness for wireless power transfer technology.

There are two major technical challenges to address the considered problem. The first technical challenge is that guaranteeing any point over the charging area under EMR safety threshold causes infinite constraints, which is an intractable problem. The second technical challenge is that distributed algorithms or partially distributed algorithms with low computation cost at each node are desired due to the potential large size of wireless sensor networks.

For the first problem, we employ the area discretization method to transform infinite constraints into finite constraints. For the second problem, we propose two algorithm to tackle it. One is a semi-distributed algorithm, named by Primal-Dual algorithm. We adopt lagrangian dual method to transform constrained nonlinear convex optimization problems into unconstrained convex optimization problem and the complex problem is decomposed into primal problem and subproblems, which are easier to address. As one target function of the subproblems is not strictly convex and non-differentiable which invalidates traditional gradient methods, we use sub-gradient algorithm instead of gradient method to solve the reformulated problem. The algorithm is semi-distributed in the sense that it needs a network-wide information dissemination at each

iteration. The other is a fully distributed algorithm, named by area division algorithm. The basic idea of the algorithm is as follows. First, it proposes a kind of scheduling policies that partition the whole area into subareas, and switch off the chargers lying on the boundaries of these subareas such that we can safely consider the optimization problem in each subarea independently. Then, it enumerates a fixed number of such scheduling policies and forges a final scheduling scheme based on these policies. The algorithm is fully distributed in that it is performed on each charger and merely requires related information from surrounding chargers within a certain distance. Moreover, we prove that the algorithm achieves $(1-\epsilon)$-approximation ratio.

We conducted extensive simulations and field experiments to verify our two algorithms. The simulation results show that our algorithms outperform one comparison algorithm by more than 37%, and are very close to another comparison algorithm, which is centralized and has the optimal results, in terms of error threshold ϵ, iteration number, EMR threshold R_t, device number. The field experimental results show that all the EMR values in the area are below a given threshold R_t and the charging utilities are consistent with the simulation results.

II. Related Work

Energy efficiency issue concerning electromagnetic radiation (EMR) safety for wireless power transfer has received more and more attention over the past few years. Dai *et al.* [14] raised EMR safety problem for the first time and studied the energy efficiency problem under EMR safety guarantee in wireless sensor networks, and further explored the issue for adjustable chargers in [15]. [14] and [15] studied maximizing the overall utility of all devices, while we focus on maximizing the minimum utility for all devices under EMR safety guarantee. In [16], Dai *et al.* studied the fundamental issue of wireless charger placement with EMR safety constraint. They also investigated the wireless charging task scheduling with the same constraint in [17]. In [18], Sotiris *et al.* aimed to optimize the efficiency of wireless energy transfer under EMR constraints and achieve good trade-offs between charging efficiency and radiation level.

III. Problem Statement

A. System Model

Consider a wireless charging network distributed in a 2D plane with n identical stationary wireless power chargers $S = \{s_1, s_2, \ldots, s_n\}$ and m rechargeable devices $O = \{o_1, o_2, \ldots, o_m\}$. We assume that the power level of chargers is adjustable and the adjusting factors x_i can continuously change from 0 to 1. A charger has maximum power value with $x_i = 1$. The rechargeable devices maintain normal working by harvesting wireless power originated from the chargers, the received power $P(d)$ by a device from a charger with distance d can be quantified by an empirical model [8], *i.e.*,

$$P(d) = \begin{cases} \frac{\alpha}{(d+\beta)^2}, & d \le D \\ 0, & d > D. \end{cases} \tag{1}$$

TABLE I
Notations

Symbol	Meaning
s_i, S	Charger i, charger set
o_j, O	Device j, device set
$P(d)$	Received power from distance d
D	Charging distance or charging radius
$d(s_i, o_j)$	Distance from charger s_i to device o_j
$d(s_i, p)$	Distance from charger s_i to point p
$u(o_j)$	Charging utility of device o_j
$e(d)$, $e(p)$	EMR from distance d, EMR at point p
x_i	Adjusting factor of charger s_i
R_t	Hard threshold of EMR safety

where α and β are known constants determined by the hardware parameters of the charger and the receiver as well as the surrounding environment, and D denotes the farthest distance a node can receive a non-zero power from the charger, which we called charging distance or charging radius. Because of hardware constraints, a device with a certain distance from the charger will fail to receive the energy. In addition, we assume the wireless power received by a node from multiple charges is additive [8], [14], [15], and the charging utility of a device is in proportion to the charging power. Then, we have

$$u(o_j) = C_1 \sum_{i=1}^{n} P(d(s_i, o_j))x_i, \tag{2}$$

where C_1 is a predetermined constant and $d(s_i, o_j)$ is the distance between the charger s_i and the device o_j.

We adopt the EMR model presented in [14] that defines the intensity of EMR to be proportional to the charging power. Then the accumulated EMR at a point p is

$$e(p) = \sum_{s_i \in S} e(d(s_i, p)) = C_2 \sum_{s_i \in S} P(d(s_i, p))x_i. \tag{3}$$

where C_2 is a predetermined constant and $d(s_i, P)$ is the distance between the charger s_i and the point p. In addition, we assume that EMR is also additive.

Table I lists the notations used in this paper.

B. Problem Definition

In this subsection, we describe our problem mathematically based on the aforementioned models.

For EMR safety, we need to ensure intensity of EMR for any point within a safe limit in the 2D plane, *i.e.*, no place will have the accumulated EMR exceeding the threshold denoted by R_t. The EMR safety guarantee can be expressed as follows

$$\forall p \in \mathbb{R}^2, \quad C_2 \sum_{i=1}^{n} P(d(s_i, p))x_i \le R_t.$$

Our goal is to maximize the minimum charging utility among all the devices to achieve fairness. Hence our problem can be defined as follows

$$\textbf{(P1)} \quad \max\min \quad C_1 \sum_{i=1}^{n} P(d(s_i, o_j))x_i$$
$$\textit{s.t.} \quad \forall p \in \mathbb{R}^2, \quad C_2 \sum_{i=1}^{n} P(d(s_i, p))x_i \le R_t,$$
$$0 \le x_i \le 1 \qquad (i = 1, \ldots, n). \tag{4}$$

IV. Problem Reformulation

As the number of constraints in problem **P1** is infinite, it is hard to find a solution to the problem. In this section, we first transform the original intractable problem with infinite constraints into a tractable one with finite constraints by using a method called area discretization [15]. Then our problem can be reformulated and become easier to solve.

In this section, we will briefly introduce the area discretization method by which constraints in our problem can be reduced in size from infinite to finite. For a detailed discussion on area discretization method, please refer to [15].

The area discretization method discretizes the 2D area by drawing K concentric circles with different radiuses for each charger. These circles split the whole network into multiple subareas as shown in Fig. 1.

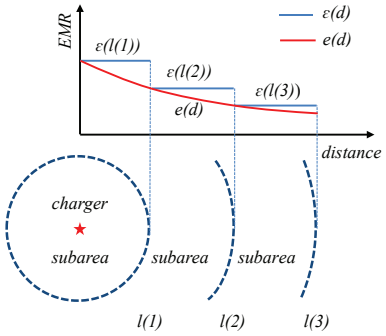

Fig. 1. Illustration of area discretization

The main procedures or conclusions of the method are listed as follows.

- The subarea faces are shaped by concentric circles and the radiuses of these circles are defined as $\ell(0) = 0$, $\ell(K) = D$, and $\ell(k) = \beta((1+\epsilon)^{k/2} - 1),\ (k = 1, ..., K-1)$ where ϵ is a pre-specified small number.
- The EMR value $e(d)$ for any position is approximated by function $\varepsilon(d)$. Furthermore, The approximated EMR for any point in the same subarea F_q are uniform. The function $\varepsilon(d)$ is defined as

$$\varepsilon(d) = \begin{cases} e(\ell(0)), d = \ell(0) \\ e(\ell(k-1)), \ell(k-1) < d \leq \ell(k)\,(0 < k \leq K) \\ 0, d > D. \end{cases} \tag{5}$$

- The approximation error of any position p in the subarea F_q satisfies

$$\frac{\varepsilon(p)}{e(p)} \leq 1 + \epsilon,\ \forall p \in F_q. \tag{6}$$

- Based on the geometry theory in [19], the number of subareas Z satisfies

$$Z = O(n^2 \epsilon^{-2}). \tag{7}$$

where n is the number of the chargers.

After the approximation procedures of area discretization, we transform the number of constraints in **P1** from infinite to finite. As a result, our original problem is reformulated as

$$\begin{aligned} \textbf{(P2)} \quad \max\min \quad & C_1 \sum_{i=1}^{n} P(d(s_i, o_j))x_i \\ s.t. \quad & C_2 \sum\nolimits_{i=1}^{n} P_{qi}x_i \leq R_t,\ (q = 1, \ldots, Z) \\ & 0 \leq x_i \leq 1,\ (i = 1, \ldots, n). \end{aligned} \tag{8}$$

where P_{qi} is the approximated power from charger s_i to the subarea F_q and Z is the total number of faces.

V. A Semi-distributed Algorithm

Consider the potential large size of wireless sensor networks, we desire distributed algorithms or at least partially distributed algorithms with low computation cost at each device. In this section, we first transform the reformulated problem into a linear program. Then, we employ lagrangian dual method to resolve our problem into the primal problem and subproblems, and use sub-gradient algorithm to solve the problem iteratively. Essentially, the whole algorithm is semi-distributed in the sense that it requires a network-wide information dissemination at the end of each iteration.

A. Problem Reformulation and Lagrangian Dual Method

Lagrangian dual method is a prevailing approach to the convex optimization problem with constraints. It is typically used to transform constrained nonlinear convex optimization problems into unconstrained convex optimization problems which are easier to be addressed. For instance, Shah-Mansouri *et al.* [20] used lagrangian dual method to lengthen work lifetime in WSN. Nevertheless, the program **P2** cannot apply Lagrangian dual method straightforwardly as its target is maximizing a minimum value, which is not a traditional optimization goal. To address this issue, we make the following reformulation to program **P2**.

We define variable E as

$$E = \min \quad C_1 \sum_{i=1}^{n} P(d(s_i, o_j))x_i. \tag{9}$$

Then problem **P2** has the following equivalent programming formulation.

$$\begin{aligned} \textbf{(P3)} \quad \min \quad & \frac{1}{E} \\ s.t. \quad & C_2 \sum_{i=1}^{n} P_{qi}x_i \leq R_t,\ (q = 1, \ldots, Z) \\ & E \leq C_1 \sum_{i=1}^{n} P(d(s_i, o_j))x_i,\ (j = 1, \ldots, m) \\ & 0 \leq x_i \leq 1,\ (i = 1, \ldots, n). \end{aligned} \tag{10}$$

The lagrangian, for $\lambda_q \geq 0$, $\nu_j \geq 0$, is given by

$$\begin{aligned} & L(E, x, \lambda, \nu) \\ =& \frac{1}{E} + \sum_{q=1}^{Z} \lambda_q (C_2 \sum\nolimits_{i=1}^{n} P_{qi}x_i - R_t) \\ & + \sum_{j=1}^{m} \nu_j (E - C_1 \sum\nolimits_{i=1}^{n} P_r(d(s_i, o_j))x_i) \end{aligned}$$

$$= -\sum_{q=1}^{Z}\lambda_q R_t + \frac{1}{E} + \sum_{j=1}^{m}\nu_j E \tag{11}$$
$$+ C_2\sum_{q=1}^{Z}\sum_{i=1}^{n}\lambda_q P_{qi}x_i - C_1\sum_{j=1}^{m}\sum_{i=1}^{n}\nu_j P_r(d(s_i,o_j))x_i.$$

The dual function is expressed as

$$\begin{aligned} g(\lambda,\nu) &= \inf_{0\le x_i\le 1,(i=1,\dots,n)} L(E,x,\lambda,\nu) \\ &= -\sum_{q=1}^{Z}\lambda_q R_t + \min(\frac{1}{E} + \sum_{j=1}^{m}\nu_j E) \\ &\quad + \min_{0\le x_i\le 1,(i=1,\dots,n)}(C_2\sum_{q=1}^{Z}\sum_{i=1}^{n}\lambda_q P_{qi}x_i \\ &\quad - C_1\sum_{j=1}^{m}\sum_{i=1}^{n}\nu_j P_r(d(s_i,o_j))x_i). \end{aligned} \tag{12}$$

Then, the primal problem of our objective is

$$\begin{aligned} \max \quad & g(\lambda,\nu) \\ \textit{s.t.} \quad & \lambda_q \ge 0,\ (q=1,\dots,Z) \\ & \nu_j \ge 0,\ (j=1,\dots,m). \end{aligned} \tag{13}$$

The two corresponding subproblems are

$$\min \quad \frac{1}{E} + \sum_{j=1}^{m}\nu_j E, \tag{14}$$

with

$$\begin{aligned} \min \quad & C_2\sum_{q=1}^{Z}\sum_{i=1}^{n}\lambda_q P_{qi}x_i - C_1\sum_{j=1}^{m}\sum_{i=1}^{n}\nu_j P_r(d(s_i,o_j))x_i \\ \textit{s.t.} \quad & 0\le x_i\le 1. \end{aligned} \tag{15}$$

B. Sub-gradient Algorithm

In this subsection, we use the sub-gradient algorithm to solve the lagrangian dual problem. However, there is a function of the subproblems that is not strictly convex and non-differentiable as well. Here we make a minor adjustment to the objective function by adding a small convex quadratic regularization term. The detailed theory and explanation can refer to [21] [22]. Specifically, we now minimize

$$\frac{1}{E} + \sigma\sum_{i=1}^{n}x_i^2. \tag{16}$$

Setting σ small enough, we can make the solution of the adjusted problem (16) arbitrarily close to the primal objective problem (9).

After adding the small convex quadratic regularization term, the Lagrange function and dual function will be updated accordingly. The updated lagrangian is given by

$$\begin{aligned} & L(E,x,\lambda,\nu) \\ &= -\sum_{q=1}^{Z}\lambda_q R_t + \frac{1}{E} + \sum_{j=1}^{m}\nu_j E + C_2\sum_{q=1}^{Z}\sum_{i=1}^{n}\lambda_q P_{qi}x_i \\ &\quad - C_1\sum_{j=1}^{m}\sum_{i=1}^{n}\nu_j P_r(d(s_i,o_j))x_i + \sigma\sum_{i=1}^{n}x_i^2. \end{aligned} \tag{17}$$

Algorithm 1 Semi-distributed Algorithm at Sink Node

INPUT Iteration number
OUTPUT Parameters in target functions

1: **while** smaller than iteration number or not meet convergence condition **do**
2: Receive $\lambda^{(k)}$ and $\nu^{(k)}$ from all devices;
3: Compute $\sum_{j=1}^{m}\nu_j^{(k)}E$, $\sum_{q=1}^{Z}\lambda_q^{(k)}P_{qi}x_i$ for $\forall i$ and $\sum_{j=1}^{m}\nu_j^{(k)}P_r(d(s_i,o_j))x_i$ for $\forall j$;
4: Compute $E^{(k)}$ in Equ. (19);
5: Broadcast $\sum_{q=1}^{Z}\lambda_q^{(k)}P_{qi}x_i$ and $\sum_{j=1}^{m}\nu_j^{(k)}P_r(d(s_i,o_j))x_i$ to the network;
6: Receive parameter $x_i^{(k)}$ from all the chargers;
7: Compute $h_q^{(k)}$ for $\forall q$, $f_j^{(k)}$ for $\forall j$ in Equ. (20);
8: Broadcast $h_q^{(k)}$ for $\forall q$, $f_j^{(k)}$ for $\forall j$ to the network.
9: **end while**

The updated dual function is expressed as

$$\begin{aligned} g(\lambda,\nu) &= \inf_{0\le x_i\le 1,(i=1,\dots,n)} L(E,x,\lambda,\nu) \\ &= -\sum_{q=1}^{Z}\lambda_q R_t + \min(\frac{1}{E} + \sum_{j=1}^{m}\nu_j E) \\ &\quad + \min_{0\le x_i\le 1,(i=1,\dots,n)}(C_2\sum_{q=1}^{Z}\sum_{i=1}^{n}\lambda_q P_{qi}x_i \\ &\quad - C_1\sum_{j=1}^{m}\sum_{i=1}^{n}\nu_j P_r(d(s_i,o_j))x_i + \sigma\sum_{i=1}^{n}x_i^2). \end{aligned} \tag{18}$$

The first sub-problem (14) remains the same, while the second sub-problem (15) is changed by adding the term $\sigma\sum_{i=1}^{n}x_i^2$.

Using the sub-gradient algorithm, the solutions of sub-problems in each iteration step are given by

$$\begin{aligned} E^{(k)} &= \arg\min(\frac{1}{E} + \sum_{j=1}^{m}\nu_j E), \\ x_i^{(k)} &= \arg\min_{0\le x_i\le 1}(\sigma x_i^2 + C_2\sum_{q=1}^{Z}\lambda_q^{(k)}P_{qi}x_i \\ &\quad - C_1\sum_{j=1}^{m}\nu_j^{(k)}P_r(d(s_i,o_j))x_i). \end{aligned} \tag{19}$$

The sub-gradients of $(\lambda^{(k)},\nu^{(k)})$ are given by

$$\begin{aligned} h_q^{(k)} &= R_t - C_2\sum_{q=1}^{Z}P_{qi}x_i \\ f_j^{(k)} &= -E^{(k)} + C_1\sum_{j=1}^{m}P_r(d(s_i,o_j))x_i. \end{aligned} \tag{20}$$

The above sub-gradients are used in the following iterative equations

$$\begin{aligned} \lambda_q^{(k+1)} &= max(0,\lambda_q^{(k)} - \alpha_k h_q^{(k)}) \\ \nu_j^{(k+1)} &= max(0,\nu_j^{(k)} - \alpha_k f_j^{(k)}). \end{aligned} \tag{21}$$

We will repeat the iterative step until the result converges, then we obtain the solution to the primal problem.

Algorithm 2 Semi-distributed Algorithm at Chargers

INPUT Initial x_i and parameters of problems
OUTPUT Solution to sub-problem $x_i^{(k)}$, $\lambda_q^{(k+1)}$ and $\nu_j^{(k+1)}$

1: Receive $\sum_{q=1}^{Z} \lambda_q^{(k)} P_{qi}$ and $\sum_{j=1}^{m} \nu_j^{(k)} P_r(d(s_i, o_j))$ from sink node;
2: Compute $x_i^{(k)}$ in Equ. (19);
3: Broadcast $x_i^{(k)}$ to the network;
4: Receive sub-gradient $h_q^{(k)}$ and $f_j^{(k)}$ from sink node;
5: Compute $\lambda_q^{(k+1)}$ and $\nu_j^{(k+1)}$ in Equ. (21);
6: Broadcast $\lambda_q^{(k+1)}$ and $\nu_j^{(k+1)}$ to the network.

C. Primal-Dual Algorithm Description

In this subsection, we present the detailed procedure for each iteration. Algorithm 1 lists the processing steps at sink node and Algorithm 2 gives the processing steps at each charger. Most of parameters, which are required for further computation in Algorithm 2, are outputs of Algorithm 1. In particular, $x_i^{(k)}$ in Step 5 for Algorithm 1 is from the output in Step 2 for Algorithm 2. The whole computation process needs the coordination between the sink node and the chargers. At each iteration, the sink node needs to collect the information from all devices for parameter computation and broadcast the results, which incurs high network-wide communication cost. Therefore, the Primal-Dual algorithm is essentially a semi-distributed algorithm, and may not be practical for real applications.

VI. A Fully Distributed Algorithm

In this section, we propose a fully distributed $(1-\epsilon)$-approximation algorithm, which is area division algorithm.

A. Key Ideas of Area Division Algorithm

The key intuitions of the area division algorithm are as follows. First, we split problem **P2** into minor ones and solve them in a distributed manner. In particular, we develop an area division scheme to divide the whole area into many subareas, and turn off the chargers lying on the boundaries of the subareas to prevent mutual interference of charging power and EMR from neighboring subareas. Thus, we can safely execute a local linear programming approach to determine the adjusting factors of the chargers in each subarea in a distributed manner. Second, to avoid the uncertainty of performance for adopting a certain area division scheme and achieve some predetermined performance bound, we consider a fixed set of area division schemes and come up with a feasible solution that achieves $(1-\epsilon)$-approximation ratio based on these schemes.

B. Description of Area Division Algorithm

First, we divide the whole area into uniform squares with size $4D * 4D$, where D denotes the farthest distance a charger can reach. Each charger and device can be easily classified into a special square according to their location and global reference anchor point. Chargers in each square then elect a square head as a delegator for computing tasks in this square. Moreover, we combine $m \times m$ squares to form a larger area, which we call m-$zone$ for short. The parameter m, which indicates the size of m-$zone$, is set as $\frac{1}{1-\sqrt{1-\frac{\epsilon}{2}}}$ to ensure the performance of the final result. For brevity, suppose that

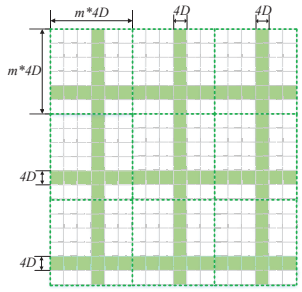

Fig. 2. Overall partition

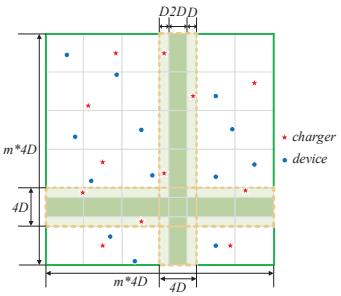

Fig. 3. m-$zone$

the whole area can be grouped into an integral number of m-$zone$s (if this is not the case, we can always achieve the goal by adding some imaginary squares).

Then, we execute a kind of area division schemes so that the whole area will be re-partitioned into some independent subareas with size at most $(m-1)\times(m-1)$ squares, which we call *new* m-$zone$s. The square heads in each new m-$zone$ also elect a m-$zone$ head as a delegator undertaking computing tasks in this m-$zone$. We formally use a tuple $< i, j >$ to denote such a scheme, or called area division policy, and perform it in the following steps. Fig. 2 shows an example for which all m-$zone$s adopt area division policy $< 5, 4 >$, and some green strips with width of $4D$ separate the whole area into 16 new m-$zone$s. Fig. 3 shows a m-$zone$ out of these 9 m-$zone$s. In this m-$zone$, the 5-th row and the 4-th column shown in colored strips of the m-$zone$ are selected and segmented into three parts. The chargers located at the central part of the row and column, or more specifically, in the dark green strips with width of $2D$ will be turned off, while the other chargers in the strips are still adjustable. Here, the $2D$ distance is sufficient to avoid the mutual influence of EMR among different new m-$zone$s and ensure applying the linear programming methods in each m-$zone$ correctly. Moreover, the devices lying in all the green strips with width of $4D$ are ignored when performing linear programming. In brief, for any $4D$ width strips, all the devices located here are ignored, but only the chargers located in the central part of strips, more precisely, in the dark green inner $2D$ width strips are switched off and the chargers located in the light green D width strips are still adjustable normally.

Apparently, there are m^2 possible area division policies (as $1 \le i, j \le m$ for any policy $< i, j >$). Different area division policies may lead to different global performance. To improve the global performance, one may consider to choose the best area division policy that yields the best performance among all m^2 ones. However, this is questionable for two reasons. First, as we switch off the chargers lying in the inner 2D width strips on the boundaries of new m-$zone$s for each area division policy, the devices that also lie in the strips may receive small or even no charging power. This contradicts our optimization goal, *i.e.*, maximizing the minimum charging for devices. Second, choosing a best area division policy needs a global knowledge about the performance for all policies as well as a global decision, which incurs a high network-wide communication cost and may be unacceptable

Algorithm 3 Fully Distributed Algorithm at Square Head

INPUT Error threshold ϵ
OUTPUT Feasible solution $(\overline{x}_1, \overline{x}_2, \cdots, \overline{x}_n)$

Initialization Phase

Let $m = \frac{1}{1-\sqrt{1-\frac{\epsilon}{2}}}$, broadcast it to all chargers to build m-$zone$s;
Elect a local square head;
Elect a local m-$zone$ head in each new m-$zone$ for each area division policy;

Working Phase

for all area division policies **do**
  Collect all the information of the chargers and devices inside the squares;
  if it is the new m-$zone$ head **then**
    Collect all the information from other square heads in the new m-$zone$;
    Equivalently "turn off" the chargers lying in the 2D strips on the boundaries and "overlook" the devices lying in the 4D strips on the boundaries, then apply the linear programming approach to compute the local optimal solution in the new m-$zone$ and obtain the adjusting factors $x_k^{<i,j>}$ for the chargers s_k in the new m-$zone$;
    Send the results to square heads in this new m-$zone$.
  else
    Receive the results from the m-$zone$ head;
    Send the results to each charger in the square;
  end if
end for
Each charger averages the adjusting factors for all the m^2 area division policies and gets a solution $\overline{x}_k = \frac{\sum_{i=1}^{m}\sum_{j=1}^{m} x_k^{<i,j>}}{m^2}$.

for real applications. To address this problem, we propose to enumerate all m^2 possible area division policies and perform linear programming method in a distributed manner for all chargers, and obtain m^2 solutions for each charger. Then, each charger averages the obtained m^2 adjusting factors and takes the final result as its adjusting factor. We will prove in the next subsection that this conduct can lead to a global feasible solution that achieves $(1-\epsilon)$-approximation ratio.

Algorithm 3 presents the pseudo-code for the area division algorithm performed at each square head. In particular, all square heads and new m-$zone$ heads can be determined in a distributed manner in the initialization phase, which can dramatically save the computation and communication overhead in the working phase, especially when the topology of the network changes in a fast speed and the working phase should be frequently invoked. Next, as shown in the for loop in the working phase, for each new m-$zone$ under each of m^2 area division policies, there is a corresponding new m-$zone$ head responsible for collecting all the information regarding chargers and devices from all square heads, computing the adjusting factors of all the chargers, and disseminating the results to all square heads which then send to their responsible chargers. When the loop completes, each charger s_k obtains m^2 adjusting factors $x_k^{<i,j>}$ $(1 \le i, j \le m)$. By averaging all the m^2 solutions, we can obtain the final feasible solution for each charger s_k, marked as $\overline{x}_k$, $(k = 1, \cdots, n)$.

C. Performance Analysis of the Algorithm

The following theorem indicates the performance of Algorithm 3.

***Theorem** 6.1: The output of the area division algorithm is a feasible solution, and the algorithm achieves $(1-\epsilon)$ approximation ratio.*

Proof: For the area division policy $< i, j >$, we have the adjusting factors for all the chargers, $x_1^{<i,j>}, \cdots, x_n^{<i,j>}$, $(1 \le i, j \le m)$. We then have

$$C_2 \sum\nolimits_{k=1}^{n} P_{qk} x_k^{<i,j>} \le R_t,$$

for any point p inside the subarea F_q.

By adding up all the inequalities for all policies together, we can obtain

$$C_2 \sum\nolimits_{i=1}^{m} \sum\nolimits_{j=1}^{m} \sum\nolimits_{k=1}^{n} P_{qk} x_k^{<i,j>} \le m^2 R_t, \tag{22}$$

and therefore,

$$C_2 \sum\nolimits_{i=1}^{m} \sum\nolimits_{j=1}^{m} \sum\nolimits_{k=1}^{n} P_{qk} \left(\frac{x_k^{<i,j>}}{m^2}\right) \le R_t. \tag{23}$$

As we set $\overline{x}_k = \frac{\sum_{i=1}^{m}\sum_{j=1}^{m} x_k^{<i,j>}}{m^2}$, we thus have

$$C_2 \sum\nolimits_{k=1}^{n} P_{qk} \overline{x}_k \le R_t, \tag{24}$$

which indicates $\overline{x}_k$ $(k = 1, \cdots, n)$ is a feasible solution to problem **P2**.

We proceed to analyze the performance of the algorithm. Let $\tilde{U}^*$ be the optimal solution for the problem **P2**. Suppose that the minimum charging utility of devices located inside the new m-$zone$s and considered in linear programming for the area division policy $< i, j >$ is $U^{<i,j>}$, and the charging utility for device $o_{j'}$ for the area division policy $< i, j >$ is $U_{j'}^{<i,j>}$. Clearly, if $o_{j'}$ is not located at the i-th row and j-th column, we have $U_{j'}^{<i,j>} \ge U^{<i,j>}$. If not, the result is uncertain. Further, as for each device located inside the new m-$zone$s and considered in linear programming, all the chargers that cover it can be freely adjusted (even for the devices lying on the boundaries of the new m-$zone$s, we still allow the chargers that lie in the light green strips as shown in Fig. 3 to cover them) and not affected by chargers from other new m-$zone$s, so we must have $U^{<i,j>} \ge \tilde{U}^*$. Consequently, we have $U_{j'}^{<i,j>} \ge \tilde{U}^*$ for devices located inside the new m-$zone$s.

In the process of looping through all m^2 area division policies, it is easy to see that for any device $o_{j'}$, there are only $2m-1$ possible cases that $o_{j'}$ lies in the i-th row or j-th column for policy $< i, j >$ and therefore has uncertain performance. In other words, in the left $m^2-(2m-1)$ cases, $o_{j'}$ must have charging utility that is greater than $\tilde{U}^*$. Then the charging utility $U_{j'}$ for $o_{j'}$ in our algorithm satisfies

$$\begin{aligned} U_{j'} =& C_1 \sum_{k=1}^{n} P(d(s_k, o_{j'}))\overline{x}_k \\ =& \frac{1}{m^2} C_1 \sum_{k=1}^{n} P(d(s_k, o_{j'})) \sum\nolimits_{i=1}^{m} \sum\nolimits_{j=1}^{m} x_k^{<i,j>} \\ \ge& \frac{1}{m^2}[m^2 - (2m-1)]\tilde{U}^* = (1-\frac{1}{m})^2 \tilde{U}^*. \end{aligned} \tag{25}$$

Further, as $o_{j'}$ is an arbitrary device, let U be the minimum charging utility in our solution, then we must have

$U \geq (1-\frac{1}{m})^2\tilde{U}^*$. As we set $m = \lceil \frac{1}{1-\sqrt{1-\frac{\epsilon}{2}}} \rceil$ as described in the initialization phase in Algorithm 3, we then have

$$U \geq (1-\epsilon/2)\tilde{U}^*. \tag{26}$$

Further, suppose that U^* is the optimal utility of the original problem **P1** and x_k^* is the adjusting factor for the charger s_k in the optimal solution. We then have

$$C_2 \sum\nolimits_{k=1}^{n} P(d(s_k,p))x_k^* \leq R_t \tag{27}$$

for any point p. Suppose the point p belongs to the subarea F_q. In particular, we set the error threshold for area discretization algorithm to $\epsilon/2$. According to Equ. (6) in the problem reformulation section, EMR at p can be approximated as

$$\varepsilon(p) = C_2 \sum_{k=1}^{n} P_{qk} x_k^* \leq (1+\epsilon/2) C_2 \sum_{k=1}^{n} P(d(s_k,p))x_k^*.$$

We immediately have

$$C_2 \sum_{k=1}^{n} P_{qk} \frac{x_i^*}{(1+\epsilon/2)} \leq C_2 \sum_{k=1}^{n} P(d(s_k,p))x_k^* \leq R_t,$$

which indicates that $\frac{x_k^*}{(1+\epsilon/2)}$ is a feasible solution for the problem **P2**.

As $\tilde{U}^*$ is the optimal solution for **P2**, we thus have

$$\begin{aligned} \tilde{U}^* &\geq \min C_1 \sum\nolimits_{k=1}^{n} P(d(s_k,o_{j'})) \frac{x_k^*}{(1+\epsilon/2)} \\ &\geq \frac{1}{(1+\epsilon/2)} \min C_1 \sum\nolimits_{k=1}^{n} P(d(s_k,o_{j'}))x_k^* \\ &\geq \frac{1}{(1+\epsilon/2)} U^* \geq (1-\epsilon/2)U^*. \end{aligned} \tag{28}$$

Combining Equ. (26) and (28), we have

$$U \geq (1-\epsilon/2) * (1-\epsilon/2)U^* \geq (1-\epsilon)U^*. \tag{29}$$

This completes the proof. ■

VII. Simulation Results

In this section, we conduct extensive simulations to evaluate the Primal-Dual algorithm and area division algorithm by comparing them with other two algorithms in terms of error threshold ϵ, iteration number, EMR threshold R_t, device number, and delay. After that, we reveal insights of the algorithms performance.

A. Evaluation Setup

We assume the chargers and devices are randomly distributed over a 2D square area. We will specify the numbers of chargers and devices respectively in each subsection. If no otherwise stated, we use the following parameter settings. We set $\alpha = 100$, $\beta = 40$ and $D = 5$ for the charging model, $C_1 = 1$ for the utility model and $C_2 = 1$ for the EMR model. The error threshold is $\epsilon = 0.5$, and the EMR threshold is $R_t = 0.08$. For the Primal-Dual algorithm, the input parameter Iteration number in Algorithm 1 is set 2000 at first for the results almost converge after 1500 iterations and will be reset 3500 when we broaden the square area to $200\,m \times 200\,m$ with more devices and chargers distributed here.

B. Baseline Setup

In our simulations, we compare our proposed algorithm with two other algorithms. The first algorithm is named by the Fminimax algorithm, which calls the fminimax procedure provided by Matlab library to solve the problem presented in our paper. The algorithm is centralized and has optimum results. The second algorithm is named by the Adjusting Factor Controlling algorithm. In the Adjusting Factor Controlling algorithm, the adjusting factors of all the chargers begin with 0 and increase by a little more in each iteration. In the whole process, the adjusting factors of all the chargers always have the same value and gradually increase simultaneously till there are EMR constraints going to be violated, then we get the final adjusting factors and the final result.

C. Performance Comparison

1) Impact of iterations number: First, we randomly scatter 15 chargers and 70 devices over a $100\,m \times 100\,m$ 2D square area with $D = 15$. As shown in Fig. 4, the Primal-Dual algorithm converges to the ending result over 1500 iterations and on average the result outperforms the Adjusting Factor Controlling algorithm, AFC in short, by 138.0%, and almost reaches 92.2% of the Fminimax algorithm. Although the Fminimax algorithm always has optimum results, it is centralized and not suitable for our networks for the considerable computing tasks. To further verify the performance of our proposed solution, we broaden the square area to $200\,m \times 200\,m$ and enlarger the number of devices to 500, and chargers to 50. As depicted in Fig. 5, the minimum utility of our proposed solution still outperforms the Adjusting Factor Controlling algorithm by 54.1%, and reaches 93.2% of the Fminimax algorithm over 2500 iterations.

2) Impact of Threshold ϵ: In this subsection, we examine the influence of the error threshold ϵ on the minimum utility, particularly focusing on area division algorithm. We scatter 150 chargers and 400 devices over a $400\,m \times 400\,m$ square area while the error threshold ϵ fluctuates between 0.05 and 0.4. As depicted in Fig. 6, the minimum utilities of Primal-Dual algorithm and Fminimax Algorithm are almost equal and relatively stable on the whole, while the utility of the area division algorithm declines with the increase of threshold ϵ. Specially, our area division algorithm is always larger than $(1-\epsilon)$ of the optimal value and outperforms the Adjusting Factor Controlling algorithm by 63.1% on average.

3) Impact of EMR Threshold R_t: We scatter 50 chargers and 200 devices in a $500\,m \times 500\,m$ square area with $\epsilon = 0.1$. As illustrated in Fig. 7, the achieved minimum utilities of the Primal-Dual algorithm and the Fminimax algorithm are close to each other. On average, the area division algorithm outperforms the Adjusting Factor Controlling algorithm by 37.7% and reaches 90.2% of the Fminimax algorithm for all the R_t values shown in the figure. The percent 90.2% is bigger than $(1-\epsilon)$ as $\epsilon = 0.1$, this verifies the Theorem 6.1 once again. The minimum utilities of the four algorithms grow with the increase of EMR threshold R_t when the R_t value is below 0.07, while the minimum utilities of our proposed algorithms and Fminimax algorithm stabilize at the peak when

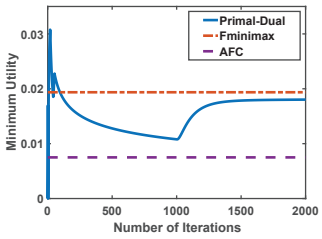

Fig. 4. Minimum utility vs. iterative number for a small-scale network

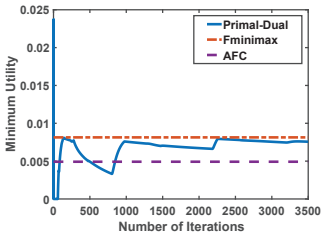

Fig. 5. Minimum utility vs. iterative number for a large-scale network

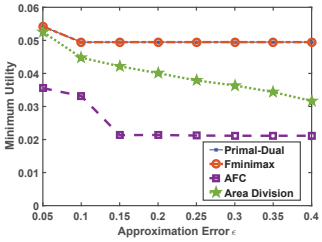

Fig. 6. Minimum utility vs. threshold ϵ

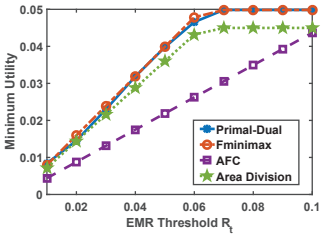

Fig. 7. Minimum utility vs. EMR threshold R_t

the R_t goes beyond 0.07. The results of the three algorithms first increase rapidly and then smoothly, and finally stabilize to a constant. This is because when the EMR threshold R_t increases to some large enough value, all the chargers in the area are adjusted to their maximum power and therefore the utility of each device will become constant.

4) Impact of Device Number: Suppose that there are 50 chargers and variable number of devices are distributed in a $500\,m \times 500\,m$ square area with $\epsilon = 0.1$. Our simulation results show that the achieved minimum utility of the Primal-Dual algorithm is almost equal to that of the Fminimax algorithm. Moreover, the area division algorithm outperforms the Adjusting Factor Controlling algorithm by 38.6% and is equal to 90.9% of the Fminimax algorithm on average. Fig. 8 shows that the minimum utilities of the four algorithms don't undergo conspicuous changes with a rise of device number. This is because if the number of devices is sufficiently large, the distance between adjacent devices would become so small that their amounts of received aggregate power are quite similar, and consequently the computed adjusting factors for all chargers don't change much and the minimum utility is relatively stable when the number of devices increases.

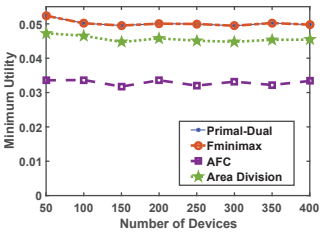

Fig. 8. Minimum Utility vs. Device Number

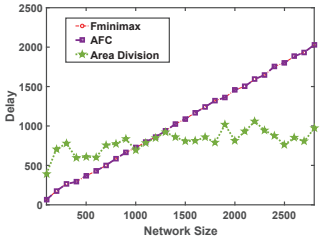

Fig. 9. Delay vs. Network Size

5) Impact of Network Size on Delay: We set the density of chargers in our area to be a constant $1/500$, and set $D = 25$, $\epsilon = 0.9$. Suppose that the communication radius is twice the charging radius, that is 50. As shown in Fig. 9, the delay of Fminimax algorithm and Adjusting Factor Controlling algorithm is nearly proportional to the network size because the two algorithms are centralized and the overall communication distances of them are closely related to the network size. In contrast, the delay of the area division algorithm merely floats in a small scale without substantial growth as the network size gets larger. The reason is that the algorithm is fully distributed and only requires local communication within a subarea, which is determined by the ϵ and isn't affected by the network size. Note that we didn't plot the delay of the Primal-Dual algorithm in Fig. 9 as it is too large, which is at least 2000 times that of Fminimax and Adjusting Factor Controlling algorithms.

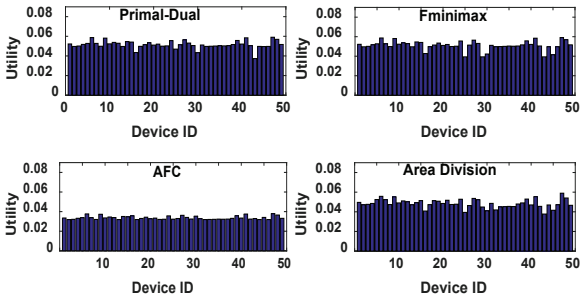

Fig. 10. Utility of devices for Four Algorithms

D. Insights

Suppose that there are 50 devices and 150 chargers deployed in a $500\,m * 500\,m$ field. We observe the utility of each of 50 devices. Fig. 10 shows the utility distribution of devices using four different algorithms. The minimum utilities are 0.03727, 0.03926, 0.03185, and 0.03772 for the Primal-Dual algorithm, Fminimax algorithm, Adjusting Factor Controlling algorithm, and area division algorithm, respectively. The results are accordant with the simulation analyses above. Besides the minimum utility, the utilities of all the devices for the four algorithms are relatively similar to each other as our problem mainly considers the fairness of charging, so the distribution of the utilities among the devices illustrates the effectiveness of our work. Among these algorithms, the utilities of devices for the Adjusting Factor Controlling algorithm appear most uniform due to the fact that it requires all the chargers sharing the same adjusting factor. Furthermore, the slight gap between our proposed algorithms and the optimum solution further validates the effectiveness of our proposed algorithms.

VIII. Field Experiments

In this section, we verify our theoretical results by implementing our scheme on a real test-bed.

A. Test-bed

The Fig. 11(a) demonstrates the test-bed that consists of two rechargeable sensor nodes and eight TX91501 power transmitters produced by Powercast [2] [23] and covers an area of $2.4\,m * 2.4\,m$. One sensor node is placed at the center of the square area and the other is on the left side of the first one with distance $0.4\,m$, while 8 power transmitters are placed on the vertices and middle points of edges of the square area, as shown in Fig. 11(a). Besides these, we utilize an access point (AP) connecting to a laptop. The AP can collect the information of the power of sensors received from the chargers

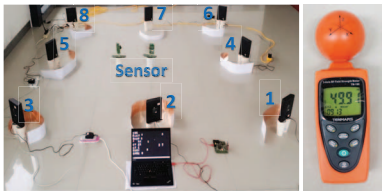

Fig. 11. Illustration of field experiment

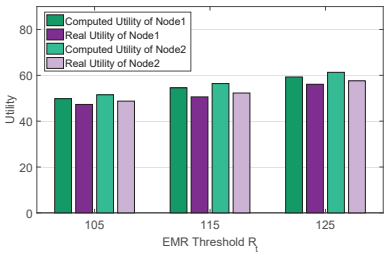

Fig. 12. Utility vs. EMR Threshold R_t

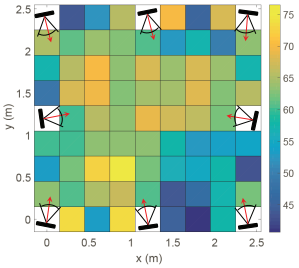

Fig. 13. An example of EMR distribution

and send this information to the laptop for data recording and analysis. Fig. 11(b) shows the RF field strength meter which we use to measure the intensity of EMR.

We place charger 1 to 8 at the predetermined angle $296.56°$, $296.56°$, $243.44°$, $26.56°$, $153.44°$, $63.44°$, $116.56°$ and $116.56°$, respectively. According to [24], [25] as well as based on our experimental results, TX91501 power transmitters are directional and their charging area can be modeled as a sector with angle $60°$ and radius $4\,m$. In addition, the power of TX91501 power transmitters is not adjustable, we approximately simulate the transmitters as adjustable by putting a piece of copper foil stripe with proper length and width in front of chargers and regulating its position and bending angle such that the intensities of power and EMR of these chargers approach a desired level.

B. Experimental Results

As Fig. 12 illustrates, we compare the utility computed based on modeling parameters with the real utility under three different R_t values to verify our area division algorithm. In particular, the modeling parameters refer to the values adopted by [15], for we use the same type of power transmitters and sensors. Especially, Node 1 refers to the sensor located at the center of the square area and Node 2 refers to the other. We can find that the minimum utility is always achieved at Node 1, and the computed utilities of both nodes are always larger than the real utility for all the R_t values, but the gap between them is small and no more than 6.5%. The gap becomes 6.3% if considering only the minimum utility. The slight difference indicates the effectiveness of our modeling approach.

The computed adjusting factors for the charger 1 to 8 are 0.68, 0.59, 0.68, 0.59, 0.59, 0.68, 0.59 and 0.68, respectively, when the EMR threshold R_t is $105\,\mu W/cm^2$. Then, we divide the square area into $9*9$ grids, sample one EMR value for each grid, and get 73 EMR values representing the grids except the locations of 8 chargers. We plot the results in Fig. 13 to show the EMR distribution over the whole area. We observe that all the EMR values in the area are less than R_t. The fact confirms the correction of our area division algorithm. Moreover, more than 83% of the EMR values in the area lie within the range of $50\,\mu W/cm^2$ and $69\,\mu W/cm^2$. This kind of EMR distribution reflects the fairness of charging power.

IX. Conclusion

In this paper, we have studied the problem of maximizing the minimum utility of devices with guaranteeing the EMR safety. We reformulated the problem by employing area discretization method. Then, we addressed the problem using two kinds of algorithms. The first named by Primal-Dual algorithm is partially distributed and the second named by area division algorithm is fully distributed and achieves $(1-\epsilon)$-approximation ratio. Finally, we conducted both extensive simulations and field experiments to evaluate the effectiveness of our proposed algorithms.

Acknowledgment

This work is partially supported by NSFC Grants (No. 61502229, No. 61373130, No. 61672276), and NSF of Jiangsu Province (No. BK20141319).

References

[1] "http://www.seattle.intel-research.net/wisp/."
[2] "www.powercastco.com."
[3] "www.powermat.com."
[4] "http://www.laptopmag.com/reviews/laptops/dell-latitude-3330.aspx."
[5] "https://en.wikipedia.org/wiki/electric_vehicle."
[6] "http://www.wareable.com/."
[7] "http://www.researchandmarkets.com/research/ft8z8p/wireless_charging."
[8] S. He *et al.*, "Energy provisioning in wireless rechargeable sensor networks," in *INFOCOM*, 2011, pp. 2006–2014.
[9] H. Dai *et al.*, "Impact of mobility on energy provisioning in wireless rechargeable sensor networks," in *WCNC*, 2013.
[10] T.-C. Chiu *et al.*, "Mobility-aware charger deployment for wireless rechargeable sensor networks," in *APNOMS*, 2012.
[11] J.-H. Liao, "Optimized charger deployment for wireless rechargeable sensor networks," 2013.
[12] R. P. Wicaksono *et al.*, "Wireless Grid: Enabling Ubiquitous Sensor Networks with Wireless Energy Supply," pp. 1–5, 2011.
[13] H. Dai *et al.*, "Quality of energy provisioning for wireless power transfer," *IEEE Transactions on Parallel and Distributed Systems*, 2014.
[14] ——, "Safe charging for wireless power transfer," in *IEEE INFOCOM*, 2014.
[15] ——, "SCAPE: Safe Charging with Adjustalbe PowEr," in *IEE ICDCS*, 2014.
[16] ——, "Radiation contrained wireless charger placement," in *IEEE INFOCOM*, 2016.
[17] ——, "Radiation constrained scheduling of wireless charging tasks," in *ACM MobiHoc*, 2017.
[18] N. Sotiris *et al.*, "Low radiation efficient wireless energy transfer in wireless distributed systems," in *IEEE ICDCS*, 2015.
[19] M. De Berg *et al.*, *Computational geometry: algorithms and applications*. Springer, 2008.
[20] V. Shah-Mansouri *et al.*, "Lexicographically optimal routing for wireless sensor networks with multiple sinks," *IEEE Tracsactions on Vehicular Technology*, vol. 58, no. 3, pp. 1490–1500, 2009.
[21] X. Lin *et al.*, "Simultaneous routing and resource allocation via dual decomposition," *IEEE Transaction on Communications*, vol. 52, no. 7, pp. 1136–1144, 2004.
[22] D. P. Bertsekas and J. N. Tsitsiklis, *Parrallel and distributed computation: numerical methods*. Prentice Hall, 1989.
[23] H. Dai *et al.*, "Near optimal charging and scheduling scheme for stochastic event capture with rechargeable sensors," in *MASS*, 2013.
[24] ——, "Omnidirectional chargability with directional antennas," in *IEEE ICNP*, 2016.
[25] ——, "Optimizing wireless charger placement for directional charging," in *IEEE INFOCOM*, 2017.